Classical kinetic theory simulations using smoothed particle hydrodynamics

James C. Simpson* and Matt A. Wood
Department of Physics and Space Sciences, Florida Institute of Technology, 150 West University Boulevard, Melbourne, Florida 32901
(Received 26 December 1995)

The technique of smoothed particle hydrodynamics (SPH) is used to simulate a variety of three-dimensional systems comprised of elastic spheres contained in a box with perfectly reflecting walls. Particle interactions are determined solely by the conservative SPH body forces, from which the potential energy function is derived. This function is followed to monitor the conservation of the total energy as various initial nonequilibrium velocity distributions are quickly randomized by particle collisions. The resulting equilibrium speed and velocity distributions are found to agree with those predicted by kinetic theory. The algorithm conserves the total energy to within 0.02%. The pressure exerted on the box walls and the mean free path between collisions are comparable with those expected for a system of rigid particles. The problem of two isolated systems that are allowed to mix after an impenetrable partition is removed is also simulated with acceptable results. Finally, the equilibrium spatial distribution of the particles is considered and a semiemperical relationship derived for this multiply anticorrelated distribution. [S1063-651X(96)01608-X].

PACS number(s): 02.70.−c, 02.70.Ns, 05.20.Dd

I. INTRODUCTION

Advances in computational science have made computer simulations an integral part of investigations of classical statistical mechanics (see [1] for a general review). The starting point for such simulations is usually the interaction potential. A number of different choices have been used, beginning with the pioneering work of Alder and Wainwright [2,3] using infinitely hard spheres surrounded by square well potentials, and followed by the introduction of the continuous Lennard-Jones potential [4,5]. In this paper we do not specify the potential *a priori*, but rather start with the fundamental fact that the momentum distributions in classical statistical mechanics do not depend on the exact nature of the interaction between the particles within a system, and so can be expressed in a form applicable to all bodies [6]. Therefore, any convenient type of interactions may be chosen for simulations of these distributions provided that no quantum effects are to be considered.

A useful computational choice turns out to be the technique of smoothed particle hydrodynamics (SPH) in which the particles may be thought of as macroscopic soft spheres (see [7] for a general review). The SPH particle interactions are repulsive and purely hydrodynamic, depending on the local pressure, density, temperature, and interparticle distance. Even though SPH has usually been used to model astrophysical situations with complicated geometries, such as mass-transferring binaries [8,9], stellar collisions [10], and the origin of the earth-moon system [11], it has many qualities that also make it well suited for basic molecular dynamics simulations.

First, the conservative and continuous SPH interparticle forces are usually truncated at a definite separation distance, avoiding the need to compute long-range forces as well as the difficulties that can be associated with discrete particle interactions such as hard spheres or square wells [12]. Second, the fundamental requirements of any SPH code to efficiently locate nearest neighbors and advance their phase-space coordinates means that it is straightforward to modify existing SPH code for simple molecular dynamics simulations [13]. Third, all the phase-space information about every particle in the system is always available for statistical analysis, so systems can be studied in considerable detail.

These are more than mere coincidences, but the simple explanation is that SPH already *is* a molecular dynamics technique that has been adapted to the needs of modeling the average properties of a fluid by using macroparticles and a smoothing procedure with a statistically significant number of neighbors (usually $\gtrsim$30 neighbors for each particle for three-dimensional systems). Hoover *et al.* [14] explore this application of SPH for molecular fluids.

But here we use SPH to simulate rarefied classical systems, so the need for a large number of neighbors is automatically eliminated, even though it is possible for any number of particles to collide simultaneously. When this does occasionally happen, the forces are just the sums due to the individual binary collisions because SPH interactions are handled pairwise. Now, if these systems are restricted to some numerical volume where wall collisions are included by reflecting the particles' normal velocities at specified boundaries, we then have an ideal method for performing simulations of classical systems governed by Maxwell-Boltzmann statistics. In the simulations presented below, we use 5000 marble-sized particles of arbitrary mass in a 1 m^3 box with perfectly reflecting walls. The particles are soft but elastic, and capable of storing elastic potential energy during collisions. We note that SPH particles do not have any spin angular momentum, so they should be regarded as smooth spheres, with only the momenta parallel to the lines joining particle centers altered during collisions.

The rest of this paper is organized as follows. In Sec. II we give a brief introduction to the theory of SPH. The details of the numerical method are given in Sec. III. The interaction potential is derived from the momentum equation in Sec. IV.

*Electronic address: simpson@hubble.pss.fit.edu, wood@kepler.pss.fit.edu

The initial, nonequilibrium velocity distributions are described in Sec. V. In Sec. VI we present the results as these systems evolve to equilibrium configurations, including the speed and velocity distributions, the pressure exerted by the particles on the walls of the box, the mean free path between collisions, and the conservation of the total energy. The basic model is then modified to simulate a mixing problem where two initially isolated systems are suddenly allowed to interact after removing a partition. We also take advantage of the SPH requirement of identifying the neighbors for each particle to measure the distribution of the number of neighbors. For comparison we derive a semiempirical analytical expression for this multiply anticorrelated distribution. Finally, we conclude in Sec. VII with a summary of our results and some suggestions for other applications of this new use of SPH.

II. SPH FUNDAMENTALS

The method of smoothed particle hydrodynamics is a Lagrangian technique first developed to model astrophysical problems with complicated geometries [15,16]. The fluid is assumed to consist of a finite number of fluid elements, and the local fluid properties at position $\mathbf{r}$ are determined by sampling nearby fluid elements and weighting their contributions according to an analytic *smoothing kernel* that smooths (or averages) local fluctuations.

The fluid elements are assumed to be spherical particles of effective radius h, and the kernel is usually chosen so that the sampling includes only those particles within $2h$ of a given point in space; consequently, the quantity h is also known as the *smoothing length*. We assume that all particles have equal mass and that h is equal for all particles and constant in time.

The smoothed interpolant for a physical field $A(\mathbf{r})$ is given by

$$\langle A(\mathbf{r})\rangle = \int A(\mathbf{r}')W(\mathbf{r}-\mathbf{r}',h)d\mathbf{r}', \tag{1}$$

where $W(\mathbf{r},h)$ is the smoothing kernel and the integration is over the entire space in which the kernel is defined. The function $W(\mathbf{r},h)$ is chosen to be differentiable and sharply peaked so that it resembles a δ function as $h\to 0$, and is normalized such that $\int W\, dV=1$.

The smoothing kernel used throughout this work is

$$W(r_{ij},h)=\frac{1}{\pi h^3}\begin{cases} 1-\frac{3}{2}q^2+\frac{3}{4}q^3 & \text{if } 0\leqslant q\leqslant 1,\\ \frac{1}{4}(2-q)^3 & \text{if } 1\leqslant q\leqslant 2,\\ 0 & \text{otherwise,}\end{cases} \tag{2}$$

where $q=r_{ij}/h$ and the factor $1/\pi h^3$ is the normalization constant [17]. Interparticle distances are discretized with 400 increments per h, and nearby particles are located using the sorting routine described by Simpson [18].

If $W(\mathbf{r})$ is an even function, then $A(\mathbf{r})=\langle A(\mathbf{r})\rangle+O(h^2)$. Hence, any physical field can always be replaced by its smoothed estimate to within the accuracy of the smoothing process. In SPH, all physical fields are replaced by their smoothed interpolants and the angular brackets are dropped as a matter of convenience. Furthermore, because we must assume a finite number of fluid elements, the integral in Eq. (1) is replaced by a summation over all the particles within $2h$ of the location $\mathbf{r}$. This procedure yields the general form of SPH interpolants:

$$A(\mathbf{r})=\sum_j m_j\frac{A_j}{\rho_j}W(\mathbf{r}-\mathbf{r}_j,h), \tag{3}$$

where m_j is the mass of the jth nearest neighbor. For example, the interpolated density for particle i is

$$\rho_i=\sum_j m_j W_{ij}. \tag{4}$$

Spatial derivatives of interpolated quantities may be found in a similar manner by using

$$\nabla A(\mathbf{r})=\sum_j m_j\frac{A_j}{\rho_j}\nabla W(\mathbf{r}-\mathbf{r}_j,h). \tag{5}$$

Usually a symmetrized form is used for derivatives by taking either the arithmetic or geometric mean of A of the particle located at $\mathbf{r}$ and particle j. Using the arithmetic mean, the momentum equation for pressure forces becomes

$$\frac{d^2\mathbf{r}_i}{dt^2}=-\sum_j m_j\left(\frac{P_i}{\rho_i^2}+\frac{P_j}{\rho_j^2}\right)\nabla_i W_{ij}, \tag{6}$$

where the sums are over all particles within $2h$ of particle i, and the gradient ∇_i is evaluated with respect to the ith coordinates.

Finally, we mention that although SPH simulations generally use some kind of artificial viscosity or damping to prevent postshock oscillations, we do not include these effects in our models because to do so would violate the spirit of the kinetic models we are simulating, even though some collisions are formally supersonic. This decision may introduce a small, but as demonstrated by the results, negligible amount of numerical noise.

III. NUMERICS

We use the isothermal equation of state

$$P_i=\rho_i c_s^2, \tag{7}$$

where c_s is the local sound speed, to guarantee that the particles' thermal energies are held constant. The collisions are therefore elastic, even though particles may actually pass through each other as discussed further in Sec. IV. It is important to note that even though the local ''pressure'' is found using an equation of state derived from kinetic theory itself, the fundamental assumption that the exact form of the particle interactions is irrelevant is not contradicted.

The momentum equation is integrated using the leapfrog method:

$$\mathbf{r}_i^n=\mathbf{r}_i^{n-1}+\Delta t^{n-1}\mathbf{v}_i^{n-1/2}, \tag{8}$$

$$\mathbf{v}_i^{n+1/2}=\mathbf{v}_i^{n-1/2}+\tfrac{1}{2}(\Delta t^{n-1}+\Delta t^n)\mathbf{a}_i^n, \tag{9}$$

where the superscripts refer to the variable time step which is chosen by

$$\Delta t^n = \epsilon \min\left[\frac{h}{v_{\max}^{n-1/2}}, \left(\frac{h}{a_{\max}^n}\right)^{1/2}, \frac{h}{c_s}\right]. \tag{10}$$

The subscript ''max'' refers to the maximum value of all particles and $\epsilon=0.3$ is the Courant number [19] chosen to maintain numerical stability. A typical time step for the models presented in this paper is $\approx 3\times 10^{-6}$ s.

The walls of the box holding the particles are assumed to be flat and perfectly reflecting. The calculation of collisions between the particles and the walls requires the end point velocities, which are found by

$$\mathbf{v}_i^n = \tfrac{1}{2}(\mathbf{v}_i^{n+1/2} + \mathbf{v}_i^{n-1/2}). \tag{11}$$

If a particle is approaching a wall and is within h of the wall, the normal component of the velocity is reflected by

$$\mathbf{v}_{i,\text{normal}}^{n+1/2} = \mathbf{v}_{i,\text{normal}}^{n+1/2} - 2\mathbf{v}_{i,\text{normal}}^{n}. \tag{12}$$

This method of handling wall collisions is quite different from the usual method of modeling boundaries by dense arrays of SPH particles [14], and can be extended to arbitrarily shaped surfaces provided that the local normal is known.

As noted above, the actual mass m of the particles is arbitrary and irrelevant if we assume that the mass of the box is much greater than m and that the particles are identical and only interact with each other. Consequently, we use units of energy and pressure *per unit mass*. In MKS units, these are $\text{m}^2\,\text{s}^{-2}$ and $\text{m}^{-1}\,\text{s}^{-2}$, respectively.

It is convenient to use velocities in units of the local isothermal sound speed when considering the total kinetic energy. For all the simulations presented we use $c_s=\sqrt{kT/m}$ $=200$ m/s, and note that the temperature and mass could be specified, if desired. The total kinetic energy (per unit mass) for a system of N particles is then $\frac{3}{2}NkT/m=\frac{3}{2}Nc_s^2$. The numerical integration scheme conserves this to within $\approx 0.02\%$ over $\simeq 10^5$ time steps. The results were all generated on a Sparc ELC using FORTRAN 77 with single precision numbers, typically requiring ~ 3 h of CPU time per 0.1 s of simulated time.

IV. THE POTENTIAL ENERGY FUNCTION

The fact that the SPH forces are conservative allows us to derive the potential energy function from the equation of motion. For a single pair of equal mass particles the accelerations are given by Eq. (6),

$$\mathbf{a}_i = -\mathbf{a}_j = -\left(\frac{P_i}{\rho_i^2} + \frac{P_j}{\rho_j^2}\right)\boldsymbol{\nabla} W_{ij}(q) = -\boldsymbol{\nabla} u_{ij}, \tag{13}$$

where u_{ij} is the elastic potential energy per unit mass of the collision. Using Eq. (7) we obtain

$$2c_s^2\left(\frac{\boldsymbol{\nabla}' W_{ij}(q)}{1+W'_{ij}(q)}\right) = \boldsymbol{\nabla} u_{ij}(q). \tag{14}$$

The notation W' indicates that the normalization constant is *not* to be included. Integrating Eq. (14) gives

$$u_{ij}(q) = 2c_s^2 \ln[1+W'(q)]. \tag{15}$$

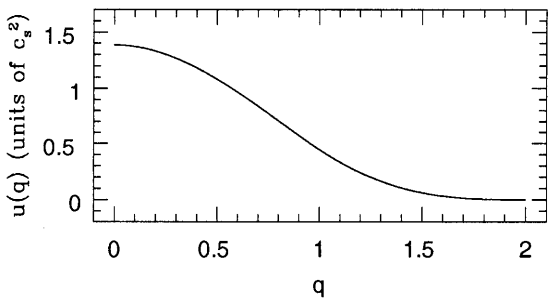

FIG. 1. The potential energy equation (15) as a function of particle separation for one pair of colliding particles.

This function is shown in Fig. 1 using W as given in Eq. (2). The maximum potential energy of a binary collision is $(2\ln 2)c_s^2 = 1.38c_s^2$. If the total kinetic energy of a colliding pair exceeds this value, the particles will pass through each other. This certainly occurs in these simulations because some particles have speeds several times c_s. The total potential energy U^n of the entire system at time step n is then

$$U^n = 2c_s^2 \sum_i \ln\left(1+\sum_j W'(q_{ij})\right), \tag{16}$$

where $1+\Sigma W'(q_{ij})$ is the number density at the location of particle i. This basic result is mentioned briefly in [20].

Even though it is not strictly necessary, we also integrate the the internal energy equation for each particle as a check on the numerical stability of our models and for comparison with Eq. (16). The standard hydrodynamic equation for the rate of change of the internal energy due to body forces is

$$\frac{du_i}{dt} = -\frac{P_i}{\rho_i}\,\boldsymbol{\nabla}\cdot\mathbf{v}_i, \tag{17}$$

which can be written in SPH formalism as

$$\frac{du_i}{dt} = \frac{P_i}{\rho_i^2}\sum_j m\mathbf{v}_{ij}\cdot\boldsymbol{\nabla}_i W_{ij}, \tag{18}$$

where $\mathbf{v}_{ij}=\mathbf{v}_i-\mathbf{v}_j$. We integrate this with the simple one-step implicit method,

$$u_i^n = u_i^{n-1} + \Delta t^{n-1}\,\frac{du_i^n}{dt}, \tag{19}$$

and set $u_i=0$ when there are no nearest neighbors. The total integrated potential and kinetic energies at time step n are then

$$U^n = \sum_i u_i^n \tag{20}$$

and

$$K^n = \frac{1}{2}\sum_i \mathbf{v}_i^n\cdot\mathbf{v}_i^n. \tag{21}$$

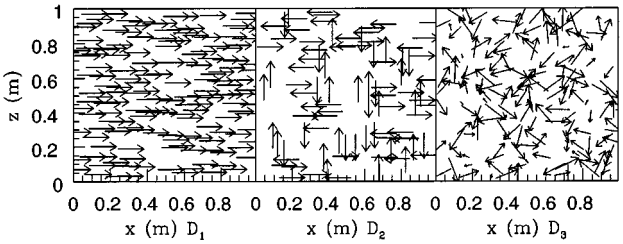

FIG. 2. The initial velocity distributions shown in the plane through the middle of the computational box. The total speed of each particle is $\sqrt{3}c_s$.

V. INITIAL CONFIGURATIONS

The models initially consist of a set of 5000, $h=0.01$ m particles placed pseudorandomly in a cube of side 1 m with initial interparticle separations of at least $4h$ and with all the particles at least $2h$ away from the walls. The total maximum volume occupied by the particles for these parameters is 0.021 m^3, satisfying the important condition that the gas be *rarefied*.

Three different initial velocity configurations are used, each of which gives every particle a total speed of $\sqrt{3}c_s$, but distributed differently between the three spatial directions so that systems with differing degrees of randomness can be compared as they approach equilibrium (Fig. 2). Particles may also be injected through a hole in one wall of the box with similar results [13]. The first initial velocity distribution, denoted D_1, gives all particles a speed of $\sqrt{3}c_s$ in the $+x$ direction. The second, D_2, randomly assigns a velocity of $\pm\sqrt{3}c_s$ in only one of the x, y, or z directions. The third distribution D_3 assigns random velocity components in all three spatial directions, with v normalized to $\sqrt{3}c_s$.

VI. RESULTS

A. Speed and velocity distributions

The distributions of the particle speeds for all three initial velocity distributions are shown in Fig. 3 as the systems come to equilibrium. As expected, these rapidly approach the theoretical Maxwell-Boltzmann curves, regardless of the initial velocity distribution. The initially more randomized distributions D_2 and D_3 approach the expected curves slightly faster than D_1. Each of these systems is well randomized and close to equilibrium after ~50 collisions per particle, and they are close to Maxwellian after as few as ~25 collisions, with D_2 and D_3 requiring only about 15 to 20 collisions. The speed distributions are nearly identical after ~0.02 s.

The collision rate of ~25 collisions per particle per 0.01 s of real time was found to be approximately constant as all three systems were followed out to a maximum of 0.3 s real time. The method of measuring the number of collisions is described in the next section.

In Fig. 4 we show the distribution of speeds as well as velocities for D_1 averaged over several different times after equilibrium has been established. The theoretical curves are again shown for comparison. There are slight deviations due to random fluctuations which are most pronounced near the peaks, but in general there is excellent agreement. The results for D_2 and D_3 are similar.

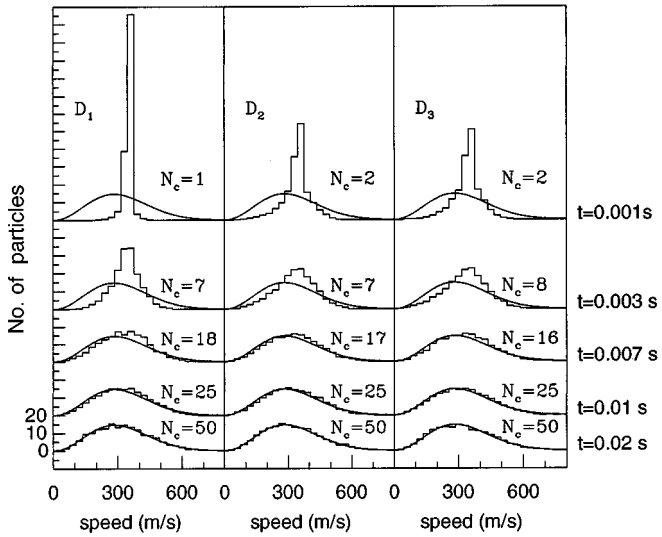

FIG. 3. Histograms of the particle speeds as the systems approach equilibrium. The exact theoretical Maxwell-Boltzmann distributions are shown for comparison. The average number of collisions per particle is also given for each time.

B. Collisions and mean free paths

The expected mean free path λ for a system of N identical *hard-sphere* particles of radius r contained inside a volume V can be derived by scaling arguments [21] and is

$$\lambda_{\mathrm{HS}}=\frac{V}{4\sqrt{2}\pi r^2 N}. \tag{22}$$

For the parameters used here, $\lambda_{\mathrm{HS}}=0.113$ m.

We measure λ_{SPH} for each particle by assuming that each free path begins when the particle no longer has any neighbors, and ends when it first contacts another particle. These

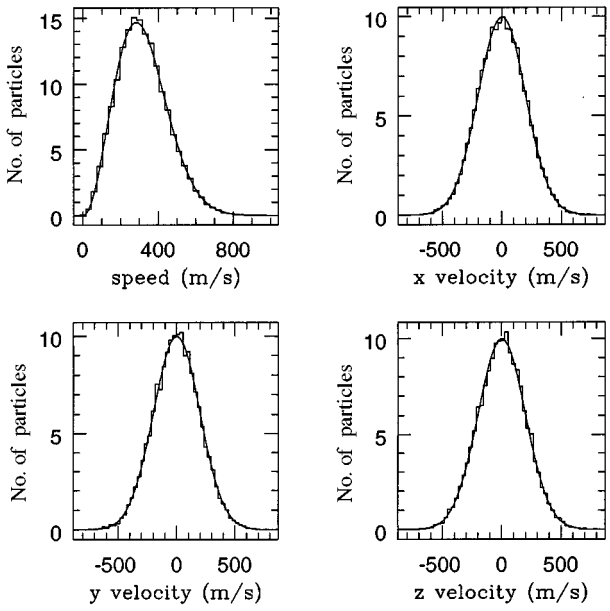

FIG. 4. Speed and velocity distributions for D_1 averaged over the five different times $t=0.1$, 0.15, 0.2, 0.25, and 0.3 s.

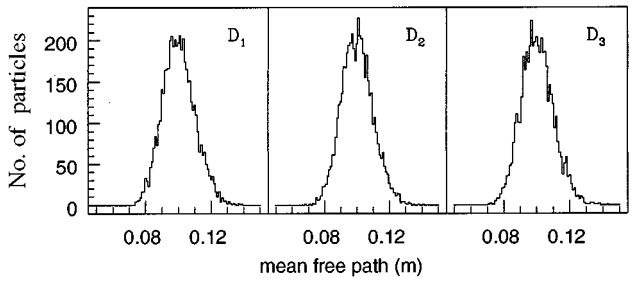

FIG. 5. Histograms of the mean free paths for all particles between $t=0.1$ and 0.2 s for each initial velocity distribution.

distances are summed and then divided by the number of collisions to find the mean free path for each particle. Multiple particle collisions are not handled in any special manner—a particle is either colliding or it is not. So even though a particle may collide with several particles either simultaneously or sequentially and register only the end of the most recent free path, no free path distance is recorded until the particle once again has no neighbors.

The histograms of the individual mean paths for all three initial distributions for the time interval between 0.1 and 0.2 s are shown in Fig. 5. These are basically Gaussians skewed very slightly towards the larger values, with virtually identical average values of 0.100 ± 0.010 m.

The value for λ_{HS} is within about one standard deviation of λ_{SPH}, which is also h. The most obvious reason for this difference is that SPH particles are *not* hard spheres but can interpenetrate after first coming into contact with each other and before reversing their direction. Figure 6 shows the average interparticle distance for each colliding particle for D_1 at $t=0.2$ s. Although it is clear that most of these distances are greater than $1.5h$ (0.015 m), about 30% are less, indicating that substantial particle interpenetration occurs. This means that when a collision is recorded and the free path calculated, the distance is underestimated by a maximum amount of about h. The relatively small number of particles in the systems is also a factor in these different values for λ, with the difference being inversely proportional to the number of particles.

C. Pressures

The expected pressure that the particles exert on the walls of the box due to momentum transfer is

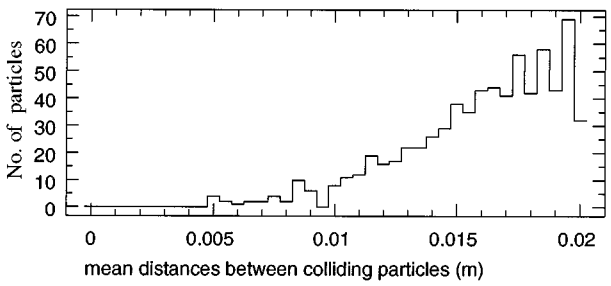

FIG. 6. The histogram of the distances between colliding particles for D_1 at $t=0.2$ s.

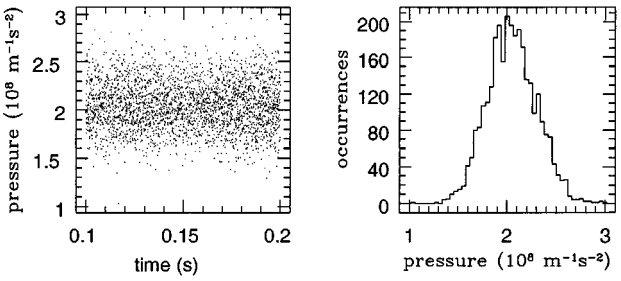

FIG. 7. Pressure vs time and a histogram of the pressures for D_1 during the time interval between 0.1 and 0.2 s.

$$P=\frac{1}{3}\frac{N}{V}m\overline{v^2}, \tag{23}$$

where $\overline{v^2}=3c_s^2$. We expect a value of 2×10^8 m^{-1} s^{-2} for $N=5000$, $V=1$ m^3, and $c_s=200$ m/s.

The pressure at the end of each time step is measured by summing the absolute values of the change in the normal velocities reflected when wall collisions occur and dividing this by the time step. These pressures are then averaged over every 10 time steps between 0 and 0.3 s. The pressures for each of the initial velocity distributions are nearly identical and constant over sufficiently long intervals ($\gtrsim$0.01 s).

The pressures for D_1 during the time interval from 0.1 to 0.2 s are shown in Fig. 7. The results for other time intervals and also for D_2 and D_3 are nearly identical and are not shown. The pressure vs time plot shows random fluctuations about a constant mean value, while the histogram is a broad Gaussian with considerable fluctuations caused by the fact that, on average, only $\sim$10 particles collide with the walls each time step. In system units, the pressure varies from about 1×10^8 to 3×10^8 with an average of 2.049×10^8 and a rms deviation of 2.50×10^7. The average pressure is 2.45% larger than expected because any particle approaching and within h of a wall is reflected, resulting in a smaller than average particle density near the walls. This effectively decreases the volume of the box by $\sim$6% for particles approaching the walls, but not for particles receding from the walls. The net result is about a 3% decrease in the volume of the box, and hence an increase in the pressure by about the same amount by Eq. (23), in reasonable agreement with the simulated results.

D. Conservation of energy

Because these are simulations and not actual physical systems, the energy does not fluctuate as it would for a real isothermal system in contact with a very large heat reservoir. Consequently, the total energy should be very nearly constant if the integration schemes are sound. The total energy for all models is conserved to within 0.02% over some 10^5 time steps using either Eq. (16) or (20) with Eq. (21), but the logarithmic potential Eq. (16) artificially reduces the dispersion in the total energy because it is slightly out of phase with the velocities used to find the total kinetic energy at time step n. This tends to cancel the random errors and reduce the dispersion in the total energy by a factor of about 4 or 5 as demonstrated in Fig. 8 during the first 0.03 s for D_1. This plot also shows some ringing during the beginning of

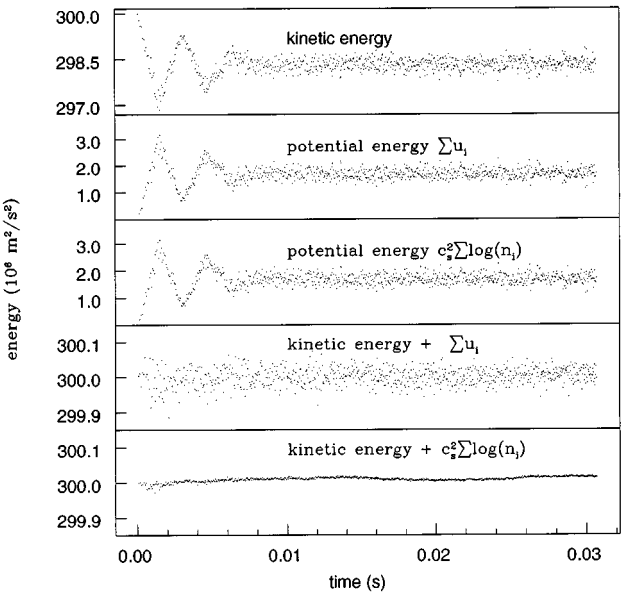

FIG. 8. The kinetic, potential, and total energies for D_1 during the first 0.03 s. The ringing at the start is due to the uniform initial velocities.

the simulation because each particle has the same velocity and no nearest neighbors. This is not seen in the energy plots for D_2 and D_3 (not shown).

E. Isothermal mixing

The models we have presented are easily modified to handle mixing problems, so we now consider two containers initially at equilibrium with the same number of particles with the same total energy ($T_1=T_2$), but at different pressures ($V_1\neq V_2$) [6]. The containers are then joined and the particles allowed to mix. The final expected pressure after the mixed system comes to equilibrium is

$$P=2\left(\frac{1}{P_1}+\frac{1}{P_2}\right)^{-1}. \tag{24}$$

We use D_1 for this test and two different sized containers, each with 5000 particles and a particle sound speed of $c_s=200$ m/s. One container (V_1) is a 1 m^3 cube, and the other container (V_2) is a box with linear dimensions $0.8\times1\times1$ m^3. The measured pressures (in system units) for each subsystem just before joining them are 2.049×10^8 for V_1 and 2.569×10^8 for V_2, giving an expected final pressure of 2.279×10^8. We measure the final pressure averaged over every 10 time steps during the 0.2 s interval after joining the boxes and obtain excellent agreement with a mean value of 2.276×10^8 and a rms deviation of 2.25×10^7. The momentum distributions of the mixed system are also found to agree with the theoretical distributions and are not shown.

F. Distribution of the number of neighbors

Because a fundamental requirement for SPH calculations is the determination of all other particles within $2h$ of any given particle, we know the number of neighbors that any particle has at the end of any time step and can compare the corresponding simulated and theoretical distributions. It is worthwhile to briefly describe an approximate analysis for determining the number of neighbors that any particle is expected to have while paying special attention to the assumptions used [6].

TABLE I. The theoretical and simulated distributions of neighbors.

Number of neighbors (n)	Theoretical no. of particles	Simulated no. of particles
0	4286.0	4289.6
1	660.4	659.9
2	50.9	47.7
3	2.6	2.2
4	0.1	0.07

Let V and N be the volume occupied by the gas and the number of particles in it, and v a small part of the volume, $v\ll V$. If the gas is assumed to be uniform and the particles *noninteracting*, the probability that that any given particle is in the volume v is v/V, so that the probability that n given particles are in this volume is $(v/V)^n$. Similarly, the probability that a particle is not in v is $(V-v)/V$, and the probability that $N-n$ given particles are not in this volume is $[(V-v)/V]^{N-n}$. If we include a factor which gives the number of ways of choosing n out of N particles, then for N large and $n\ll N$, the probability $P(n)$ that v contains n particles becomes the Poisson distribution,

$$P(n)=\frac{\alpha^n e^{-\alpha}}{n!}, \tag{25}$$

where $\alpha=Nv/V$.

But this is not the situation that we have because the particles *do* interact and are moving. Furthermore, we want the distribution of the number of neighbors the particles have, and not the number density at some random location in the volume V. This second difference is easy to resolve. Because a particle can have at most $N-1$ neighbors, it only necessary to replace N by $N-1$ in Eq. (25). The total number of particles with n neighbors is then

$$NP(n)=\frac{N\alpha^n e^{-\alpha}}{n!}, \tag{26}$$

where now $\alpha=(N-1)v/V$.

The fact that the particles interact and are moving is a more complicated issue. The particle interactions are repulsive, so we expect the actual number of particles with n neighbors to be less than that given by Eq. (26). The simplest way to account for this is to replace v in this equation by an effective volume $v_*<v$, and then to determine v_* *empirically* such that the results from Eq. (26) agree with the simulated results. The results for $v_*=0.92v$ (corresponding to an effective maximum interaction distance of $h_*=0.019\,45$) are shown in Table I for D_1.

This is an admittedly crude, although intuitive, first-order approximation to the complex issue of n-point anticorrelation functions as discussed in depth by Peebles [22]. We have circumvented most of the complexity by choosing only *one* effective volume for any number of neighbors. This vol-

ume was chosen to make the $n=2$ values agree closely, so the agreement between the simulated and analytical values decreases steadily for larger n.

VII. CONCLUSIONS

We have demonstrated that the numerical technique commonly known as SPH can be easily modified for simple molecular dynamics simulations of systems confined inside containers with perfectly reflecting walls. Regardless of the initial velocity distribution, collisions quickly redistribute the momenta so that the speed and velocity distributions become Maxwellian by the time each particle has undergone ~ 50 collisions with other particles. For the parameters used here, the mean free paths differ by $\sim 10\%$ from those predicted for a system of hard spheres because substantial particle interpenetration occurs. The pressure exerted on the container walls due to momentum exchange with the particles agrees with the predicted values to within $\sim 3\%$, while the time integration scheme conserves the total kinetic energy to within about 0.02% over some 10^5 time steps. A basic mixing problem of two isolated equilibrium systems that are suddenly allowed to interact gives excellent agreement between the expected and simulated system pressures. Finally, the spatial distribution of the particles can be measured and compared to a simple theoretical n-point anticorrelated distribution by defining an effective interaction volume.

There are many ways these basic simulations can be modified to handle more complicated and practical problems. We have used isothermal particles, but heat transfer between particles requires only a different equation of state and a more accurate integration scheme for the energy equation. There can also be heat transfer between the particles and the walls if a thermal conduction term is added to the energy equation. Although we have restricted ourselves to identical mass and size particles for simplicity, this can be changed to model nonhomogeneous systems. It is trivial to include external force fields, if desired. The flat walls can be replaced by arbitrary surfaces if the local normal vectors are known.

Other types of physical systems can also benefit from the general numerical techniques that SPH uses. These include any type of systems where the particle interactions act over short, well-defined ranges, such as the motion of ions in a heavily screened potential. For this particular example the SPH forces would need to be replaced by Coulombic forces, but the general SPH sorting and integration schemes could be used with few, if any, changes.

[1] F. F. Abraham, Adv. Phys. **35**, 1 (1986).
[2] B. J. Alder and T. E. Wainwright, J. Chem. Phys. **33**, 1439 (1960).
[3] B. J. Alder and T. E. Wainwright, J. Chem. Phys. **31**, 459 (1959).
[4] A. Rahman, Phys. Rev. **136**, A405 (1964).
[5] L. Verlet, Phys. Rev. **159**, 98 (1964).
[6] L. D. Landau and E. M. Lifshitz, *Statistical Physics*, 3rd ed. (Pergamon, Oxford, 1980).
[7] J. J. Monaghan, ARA&A, **30**, 543 (1992).
[8] D. Molteni, G. Belvedere, and G. Lanzafame, Mon. Not. R. Astron. Soc. **249**, 748 (1991).
[9] Z. Meglicki, D. Wickramasinghe, and G. Bicknell, Mon. Not. R. Astron. Soc. **264**, 691 (1993).
[10] J. Goodman and L. Hernquist, Astrophys. J. **378**, 637 (1991).
[11] W. Benz, W. L. Slattery, and A. G. W. Cameron, Icarus **66**, 515 (1986).
[12] M. P. Allen and D. J. Tildesley, *Computer Simulation of Liquids* (Clarendon, Oxford, 1987).
[13] J. C. Simpson, Ph.D. dissertation, Florida Institute of Technology, 1995.
[14] W. G. Hoover, T. G. Pierce, C. G. Hoover, J. O. Shugart, C. M. Stein, and A. L. Edwards, Comput. Math. Applic. **28**, 155 (1994).
[15] L. Lucy, Astron. J. **82**, 1013 (1977).
[16] R. A. Gingold and J. J. Monaghan, Mon. Not. R. Astron. Soc. **181**, 375 (1977).
[17] J. J. Monaghan and J. C. Lattanzio, Astron. Astrophys. **149**, 135 (1985).
[18] J. C. Simpson, Astrophys. J. **448**, 822 (1995).
[19] W. H. Press, B. P. Flannery, S. A. Teukolsky, and W. T. Vetterling, *Numerical Recipes: The Art of Scientific Computing* (Cambridge University Press, Cambridge, England, 1986).
[20] R. A. Gingold and J. J. Monaghan, J. Comput. Phys. **46**, 429 (1982).
[21] J. F. Lee, F. W. Sears, and D. L. Turcotte, *Statistical Thermodynamics*, 2nd ed. (Addison-Wesley, Reading, MA, 1973).
[22] P. J. E. Peebles, *The Large-Scale Structure of the Universe* (Princeton University Press, Princeton, NJ, 1980).